

Preliminary Results on the Multiplicity in π -Nucleus Interactions at 100 and 175 GeV/c, and Models of the Space-Time Development of Particle Production*

W. Busza, J. Elias⁺, D. Jacobs, M. Sogard[†], P. Swartz, and C. Young

Physics Department and Laboratory for Nuclear Science
Massachusetts Institute of Technology

ABSTRACT

A novel Cerenkov counter technique has been used to measure charged particle multiplicity in π^- - Nucleus collisions at 100 and 175 GeV/c. The results are: a) In the forward direction the multiplicity is independent of the target nucleus; b) In the backward direction (in the πp c.m. system) the multiplicity is approximately proportional to the nuclear thickness; and c) The data are consistent with the assumption that the relevant parameter which describes the multiplication process is the absorption cross-section of the incident particle rather than that of the produced secondaries. The results are in excellent agreement with Gottfried's model of the space-time development of particle production.

+ Present address: Fermi National Accelerator Laboratory, Batavia, Illinois

† Present address: Laboratory of Nuclear Studies, Cornell University, Ithaca, New York

* Invited paper presented by W. Busza at the Topical Meeting on High Energy Collisions Involving Nuclei, Trieste, 8-14 September, 1974.

Work Supported in part through funds provided by the U.S. Atomic Energy Commission under Contract No. AT (11-1)3069.

Introduction

Experiments on multiparticle production using nucleons as targets give data only on the asymptotic states produced and thus cannot yield direct information on the space-time development of the production process. A study of correlations in the asymptotic states can provide this information but only indirectly. In order to study the evolution of the production process it is necessary to interfere, in a controlled manner, with the process while it is taking place. Reasonable estimates¹ indicate that at FNAL energies hadronic interactions take place over distances of many fermis in the laboratory frame of reference, i.e., in distances greater than the mean free path of hadrons in nuclear matter. This suggests that nuclear targets may be ideal for studying the evolution of the production process.

We have studied the development of hadronic showers inside nuclear matter, by measuring the multiplicity of charged relativistic particles as a function of angle and nuclear size in π^- -nucleus collisions.

A novel Cerenkov counter technique was used for counting the number of charged particles produced in each interaction. The experiment was carried out in the M6 beam line at the Fermi National Accelerator Laboratory.

Brief Description of the Experiment

The target in this experiment was placed at the second focus of M6, a three stage secondary beam line of 175 GeV/c maximum momentum. Four thirds of a radiation length of lead at the first

focus eliminated the few percent electron contamination in the beam. Data were taken at 100 and 175 GeV/c with a negative beam. The beam composition at 100 GeV/c was measured² to be 94.1% π^- , 4.4% K^- , 1.5% \bar{p} . At 175 GeV/c the K^- and \bar{p} contamination is known to be smaller.

The target was surrounded by a multiplicity detector consisting of twelve hodoscope counters and a high resolution Cerenkov counter in the forward direction, as shown in Figure 1. Particles produced at large angles were counted in the hodoscope counters, while those produced at small angles were counted through the pulse height in the forward Cerenkov counter. The angular range covered by the two parts of the multiplicity detector was determined by the position of the target relative to the detector. The principle of operation of the forward Cerenkov counter is illustrated in Figure 2. The detector is sensitive only to relativistic particles with $\beta \gtrsim 0.85$.

The incident beam passes through the forward detection system. Thus, to avoid two or more beam particles arriving within the resolving time of the detector, or being swamped by single particle events, it was necessary to use a selective triggering system for defining a beam particle and an inelastic event.

The beam defining telescope is shown schematically in Figure 1. Digital and pulse height information from it was used to reject all beam particles which were within 200 nsec of each other. As an extra precaution against pile-up, a beam of less than 10^5 particles/sec was used throughout the experiment.

An inelastic interaction was detected with trigger counters

which required either two or more particles in the forward direction or one at large angles in two sets of counters (see Figure 1). To avoid simulation of a real interaction by δ -rays from a non-interacting beam particle, the event trigger also required that the beam particle did not reach the third focus of the beam, i.e., that it lost at least 1 GeV.

Whenever an "Event" was detected by the trigger counters, information from the multiplicity detector was stored in one of eight separate octants of a 4096-channel pulse-height analyser (the pulse height from the forward Cerenkov counter was stored in octant #1 when no hodoscopes fired, in octant #2 when one hodoscope fired, etc). Eight octants are adequate because the probability of more than seven particles produced at angles greater than 26° , the minimum angle subtended by a hodoscope counter at the target, is negligible.

Data were collected for the following matrix of beam energies, target materials, target thickness, Cerenkov radiator thickness and angular ranges:

Beam momenta: 100 and 175 GeV/c.

Target materials: C, CH₂, Al, Cu, Ag, Pb, and U.

H₂ results were calculated from CH₂-C difference.

Target thickness: Several for each target material in range 0.25 and 6 g/cm².

Cerenkov radiators: 0.5, 1.0, and 1.5 cm at the center.

Separate angular ranges covered by the detector: 0° - 3.5° ,
 0° - 26° , 26° - 110° .

The laboratory angles of 3.5° and 26° correspond to the laboratory

pseudo-rapidity³ η of 3.5 and 1.5. The corresponding angles in the πp center of mass system for a $\beta = 1$ particle are 48° and 149° at 100 GeV/c and 61° and 156° at 175 GeV/c.

At least two runs were taken for each target. To avoid drift problems a target out run was taken between every two or three target in runs. Approximately 10^5 events were stored for each point in the multidimensional matrix.

For each run the data consist of eight pulse-height spectra as described above. One such spectrum is shown in Figure 3. In principle, after a target out subtraction, the average charged-particle multiplicity can be immediately extracted from the data by adding the average number of hodoscopes triggered to the mean multiplicity of particles passing through the forward Cerenkov counter. The mean multiplicity in the latter is given by the first moment of the pulse height spectrum divided by the first moment of the one-particle spectrum. Our trigger system rejected one-, two-, and a small fraction of three-particle events. To correct for the resulting loss of inelastic events, we first eliminated all of these events from the raw data; then, at the end of the analysis, a correction was applied for events with up to three charged particles⁴.

The statistical error on the raw multiplicities obtained is very small ($\sim 1.5\%$). Furthermore, even over long periods of time, the raw multiplicities reproduced to within these errors, indicating that no drift problems were encountered.

To extract the true multiplicities many correction factors have to be applied to the raw multiplicities. Uncertainties in

these correction factors dominate the errors. All of the important correction factors are listed below:

1) Secondary interactions in the target; i.e., extra-nuclear collisions, δ -rays and γ -conversions from π^0 's. All these processes were corrected for by extrapolating to zero target length ($\sim 6\%$ for a 1 g/cm^2 target).

2) The fact that the pulse height produced by n secondary particles is not identical to that produced by n pions of 100 GeV ($\sim 2\%$). The two differ because the multiplicity of secondary interactions in the radiator is a function of energy.

3) γ -conversion in the radiator and in the hodoscope counters ($\sim 6\%$).

4) More than one particle striking the same hodoscope counter ($\sim 5\%$).

Data from radiators of various thicknesses were used as a consistency check.

The quoted errors on our results include the uncertainties in all such correction factors, as well as the uncertainty in the correction for the one-, two-, and three-particle events. It should be noted that to a large extent the above correction factors cancel in the calculation of the ratio R_A , of the multiplicity from nuclear target A to that of Hydrogen.

Results

The method used in this experiment is new; therefore it is important, first of all, to present those results which can be compared with data obtained using orthodox techniques.

In Figure 4 we compare our measured values of the absorption cross-sections with those of Denisov et al⁵. The two are in good agreement with each other and with the power law $\sigma_A = \sigma_0 A^{0.75}$, predicted by a simple optical model calculation in which a Wood-Saxon distribution of nucleons is assumed. It shows that at high energies hadron-nucleus absorption can be described by the most naive classical picture: that of the collision between a hadron and a collection of independent nucleons each of a size equal to the single nucleon absorption cross-section.

Our preliminary values for $\langle n \rangle_{H_2}$, the average charged multiplicity of relativistic ($\beta \gtrsim 0.85$) particles in π^-p collisions at 100 and 175 GeV/c, are 6.5 ± 0.4 , and 7.7 ± 0.5 respectively. These results are to be compared with the FNAL bubble chamber measurements⁶ of 6.80 ± 0.14 , and 8.02 ± 0.12 for the multiplicity of all charged secondaries at 100 and 205 GeV/c. (The fraction of charged particles with $\beta < 0.85$ is not known, but it should certainly be less than 10%).

The most important results of the experiment are summarized in Figure 5. They confirm the old observation from cosmic ray physics⁷ and the more recent emulsion measurements⁸ at FNAL that the average multiplicity grows slowly with the atomic weight of the target, that the rise is primarily in the target fragmentation region, and that R_A is independent of energy.

Figure 5 shows the variation with nuclear size (measured in terms of \bar{v} , the average number of absorption mean free paths encountered in the nucleus by the incident particle⁹), of the observed multiplicity for the four angular regions for which we

have separate measurements. The most striking result is that there is no multiplication of particles for $\theta_{\text{lab}} < 3.5^\circ$, while at large angles the multiplicity is approximately proportional to nuclear thickness. A pion encounters on the average 3 mean free paths in a Uranium nucleus and yet for the forward cone, which contains almost half the produced particles for πp interactions, the multiplicity in a π -Uranium collision is the same as that in a π -p collision. The $\theta_{\text{lab}} > 26^\circ$ data indicates that at large angles there may be a small amount of cascading within the nucleus.

The dependence of the multiplication process on the nature of the incident particle is shown in Figure 6, where various measurements of R_A are plotted a) as a function of A and b) as a function of \bar{v} . In Figure 6b the only data shown are those for which the nature of both the incident particle and target nucleus are known. For a given value of A the value of R_A for incident pions is smaller than that for incident protons. On the other hand, comparison of our data with the world average value of R_{Em} from p-Emulsion measurements at FNAL shows good agreement when plotted as a function of \bar{v} . This comparison suggests the striking conclusion that the relevant parameter which describes the multiplication process is the absorption cross-section of the incident particle rather than that of the produced secondaries. It should be pointed out, however, that because the comparison is between very different experiments the data in this respect are not sufficient to be conclusive.

Finally in Figure 7 we show the dispersion D as a function of

average charged multiplicity $\langle n \rangle$. It is interesting to note that in π -nucleus interactions D depends linearly on $\langle n \rangle$ in the same way as in πp interactions. In neither is it Poisson-like, where $D \propto \langle n \rangle^{1/2}$.

Comparison with Theory

The observed slow increase in multiplicity with nuclear size and the energy independence of R_A rule out all cascade models¹⁰ which assume that in hadronic collisions the asymptotic multiparticle final states are formed in a distance short compared to the mean free path of hadrons in nuclear matter.

Our data are in excellent agreement with the energy flux cascade model (EFC model) of Gottfried¹¹. In our energy range, Gottfried predicts no difference in multiplicity between nuclei and Hydrogen for rapidities greater than 2.5; at 100 GeV/c we observe $\langle n \rangle_A / \langle n \rangle_{H_2}$ (for particles with $\eta > 3.5$) = $1 + (-0.005 \pm 0.050)(\bar{\nu} - 1)$, and $\langle n \rangle_A / \langle n \rangle_{H_2}$ (for particles with $\eta > 1.5$) = $1 + (0.17 \pm 0.07)(\bar{\nu} - 1)$. Gottfried predicts $\langle n \rangle_A / \langle n \rangle_H$ (all η) = $R_A = 1 + 0.38(\bar{\nu} - 1)$, independent of energy; we find $R_A = 1 + (0.43 \pm 0.05)(\bar{\nu} - 1)$ at 100 GeV/c and $R_A = 1 + (0.41 \pm 0.06)(\bar{\nu} - 1)$ at 175 GeV/c. It should be pointed out once again that the above quoted errors are not only statistical; they include all systematic effects as well as the error on $\bar{\nu}$.

The difference, if any, between our data and the EFC model can be attributed to particles produced at $\theta_{lab} > 26^\circ$, where the model is least reliable since it does not take into account the transverse development of the energy flux.

In Figure 8 we compare our results with Gottfried's model and also with $R_A = 1/2 + 1/2 \bar{v}$, a relation recently suggested by several authors¹².

To conclude, this experiment has confirmed the puzzling cosmic ray observation that there is almost no showering of hadrons inside nuclear matter. It has shown that the little intranuclear multiplication that does occur gives rise to an increase of particles only at large angles, that it is energy independent, and that it is compatible with the assumption that the absorption cross-section of the incident rather than of the produced particles determines the multiplication process. These results place severe constraints on models of multi-particle production, in particular on the space-time development of the production process. Whether the constraints will prove useful depends on how difficult it will be to interpret detailed dynamical models of high energy interactions in terms of the evolution of the production process in the presence of nuclear matter.

We thank the BNL staff for permitting us to test the detector at the AGS, and S. Redner for helping during the tests. We wish to acknowledge the aid of the FNAL staff, in particular S. Ecklund and P. Koehler. T. Lyons' technical help was invaluable throughout the experiment. We thank A. Białas, R. Diebold and K. Gottfried for many useful discussions, and B. Nelson for help in the analysis of the data.

Finally, without the constant support and encouragement of M. Deutsch, H. Feshbach, J. Friedman, H. Kendall, L. Rosenson and V. Weisskopf, the experiment never would have been started or completed.

REFERENCES

1. For example, suppose T^* is a characteristic particle production time in the center of mass frame. In the laboratory frame it will be $T = \gamma_{cm} T^* \approx (E/2M_p)^{1/2} T^*$, where E is the energy of the incident particle. The production will thus take place over a distance of $\ell \approx c (E/2M_p)^{1/2} T^*$. It is reasonable to assume that for multiparticle production $T^* \gtrsim \hbar/m_\pi$, which at 100 GeV leads to $\ell \gtrsim 10\text{fm}$. A similar value is obtained if one considers the decay of a highly unstable hadronic state of a few GeV mass and a width $\approx 1\text{ GeV}$.

2. Private communication from Experiment 96 at FNAL.

3. The laboratory pseudo-rapidity η is defined by:

$$\eta = -\ln \tan \theta_{lab}/2$$

For relativistic particles with (mass)² small compared to $\langle p_\perp^2 \rangle$, η is approximately equal to the laboratory rapidity

$y_{lab} = 1/2 \ln (E + P_{11})/(E - P_{11})$, where E and P_{11} are the laboratory energy and longitudinal momentum. For a 100 and 175 GeV/c pion beam, the πp center of mass system has $\eta = 2.7$ and 3.0 respectively.

4. In correcting for inelastic events with up to three charged prongs, the topological cross-sections were assumed to be given by $\sigma_n = \sigma_0 n^3 e^{-\mu n}$, which represents well the H_2 data. σ_0 and μ were adjusted using an iterative procedure so that, after correction, the data and the analytic function had the same mean and area. $\langle n \rangle$ is not very sensitive to the cross-sections for the production of one, two and three particles, and we estimate that the maximum error introduced by this correction procedure is less than 3%.

5. S.P. Denisov et al., NP B61, 62, (1973).
6. J. Erwin et al., PRL 32, 254, (1974).
D. Bogert et al., PRL 31, 1271, (1973).
7. M.F. Kaplon, D.M. Ritson, and W.D. Walker, Phys. Rev. 90, 716, (1953).
E. Lohrmann and M.W. Teucher, Nuovo Cimento 25, 957, (1962) and earlier references there.
E.L. Feinberg, Physics Reports 5C, #5, (1972).
A. Gurtu et al., Tata Institute report TIFR-BC-74-6 and earlier references there.
8. A. Gurtu et al., Ibid.
Barcelona-Batavia-etc. Collaboration, Phys. Lett., 48B, 467, (1974).
J. Babecki et al., Phys. Lett., 47B, 268, (1973).
9. $\bar{\nu}$ is defined as the average number of absorption mean free paths encountered in the nucleus by the incident hadron. It can easily be shown that for any nuclear distribution
$$\bar{\nu} = A\sigma_{hn}/\sigma_{hA}$$
 where A is the atomic number of the nucleus; σ_{hn} and σ_{hA} are the absorption cross-sections of the incident hadron on a nucleon and nucleus respectively. The elastic and pseudo-elastic cross-section, as well as the cross-section for the coherent production of particles should be excluded from σ_{hn} and σ_{hA} . The above formula was pointed out to us by A. Biaľas.
10. P.M. Fishbane and J.S. Trefil, Phys. Rev. D3, 238, (1971).
A. Dar and J. Vary, Phys. Rev. D6, 2412, (1972).
I.Z. Artykov, V.S. Barashenkov, and S.M. Eliseev, Nucl. Phys. B6, 11, (1968).
11. K. Gottfried, private communication and PRL 32, 957, (1974).

12. P.M. Fishbane and J.S. Trefil, Phys. Lett. 51B, 139, (1974).
G. Calucci, R. Jengo, and A. Pignotti, Phys. Rev. D (to be published), (1974).
See also:
A.S. Goldhaber, PRL 33, 47, (1974).
A. Białas and W. Czyż, Phys. Lett. 51B, 179, (1974).
L. Van Hove, invited talk at Topical Meeting on High Energy Collisions Involving Nuclei, Trieste, September, (1974).
E.S. Lehman and G.A. Winbow, Phys. Rev. D (to be published), (1974).
13. P.R. Vishwanath et al., University of Michigan report, UM-HE 74-23 (1974).
14. J. Babecki et al., Phys. Lett. 47B, 268, (1973).
K.M. Abdo et al., JINR, E1-8021, Dubna, (1974).
15. K.M. Abdo et al., Ibid.
16. P.L. Jain et al., PRL 33, 660, (1974).
Alma-Ata-etc. Collaboration, Contribution to the XVII Conference on High Energy Physics, London, (1974).
17. J.R. Florian et al., contributed paper to the Fall Meeting of the APS, Williamsburg, Virginia, 5-7 September, (1974).
18. E.L. Berger et al., CERN/D.Ph.II/Phys 74-9, (1974).
19. A. Wróblewski, compilation of Low Energy Data in Acta Phys. Pol., B4, 857, (1973).

FIGURE CAPTIONS

1. Multiplicity detector and trigger counters. $\frac{dE}{dx_1}$ and $\frac{dE}{dx_2}$ have thresholds set at 2 x (minimum ionizing).
2. Principle of the experiment.
3. A typical pulse-height spectrum. It was obtained in a 10-minute run using a 4.4g/cm^2 Al target. The spectrum contains 20,000 events.
4. πA absorption cross-section: comparison with Denisov et al⁵, and with the optical model.
5. $\langle n \rangle_A / \langle n \rangle_{H_2}$ versus \bar{v} for various angular ranges.
 $\langle n \rangle_A$ is the average charged multiplicity of relativistic particles produced in a collision with nucleus A, and \bar{v} is the average number of absorption mean free paths encountered in the nucleus⁹. Errors on \bar{v} are shown at the bottom of the graph. The errors on $\langle n \rangle_A / \langle n \rangle_{H_2}$ are statistical only. Systematic errors are as follows:

100 GeV/c	$0^\circ < \theta_{lab} < 3.5^\circ$	$\pm 6\%$
	$0^\circ < \theta_{lab} < 26^\circ$	$\pm 2\%$
	$26^\circ < \theta_{lab} < 110^\circ$	$\pm 10\%$
	$0^\circ < \theta_{lab} < 110^\circ$	$\pm 2\%$
175 GeV/c	$0^\circ < \theta_{lab} < 26^\circ$	$\pm 3\%$
	$26^\circ < \theta_{lab} < 110^\circ$	$\pm 10\%$
	$0^\circ < \theta_{lab} < 110^\circ$	$\pm 3\%$

6. Comparison of various measurements of multiplicities in hadron-nucleus collisions.

a) R_A versus A , where $R_A = \langle n \rangle_A / \langle n \rangle_{H_2}$

The Echo Lake data¹³ are an average over the energy range 80-500 GeV for incident particles consisting of approximately 30% pions and 70% protons. The 69 GeV p-Emulsion data¹⁴ and 60 GeV π^- -Emulsion data¹⁵ are from Serpukhov. The p-Emulsion data⁸ and p-Emulsion (light elements) data¹⁶ at 200 GeV are from FNAL.

Errors on all measurements are statistical only. In this comparison we have not included the very high values of R_A found by Florian et al¹⁷ in 30 p-Ag collisions and 32 p-W collisions at 300 GeV.

b) R_A versus \bar{v} for data where both the incident particle and target are well-defined. The errors include all systematic and statistical uncertainties.

7. Dispersion $D = \sqrt{\langle (n - \langle n \rangle)^2 \rangle}$ versus $\langle n \rangle$ for this experiment; the data of Berger et al¹⁸, Bogert et al⁶, and the low energy data compiled by A. Wróblewski¹⁹.

8. R_A versus \bar{v} : comparison with theory. Best fit to our data gives $R_A = 1 + (0.42 \pm 0.05)(\bar{v} - 1)$, where the error includes all systematic and statistical uncertainties. See text for a discussion of the two theoretical predictions.

$$\text{Event} \equiv \text{Beam} \cdot \left[dE/dX_1 \text{ or } W_1 \right] \cdot \left[dE/dX_2 \text{ or } W_2 \right] \cdot \bar{V}_2$$

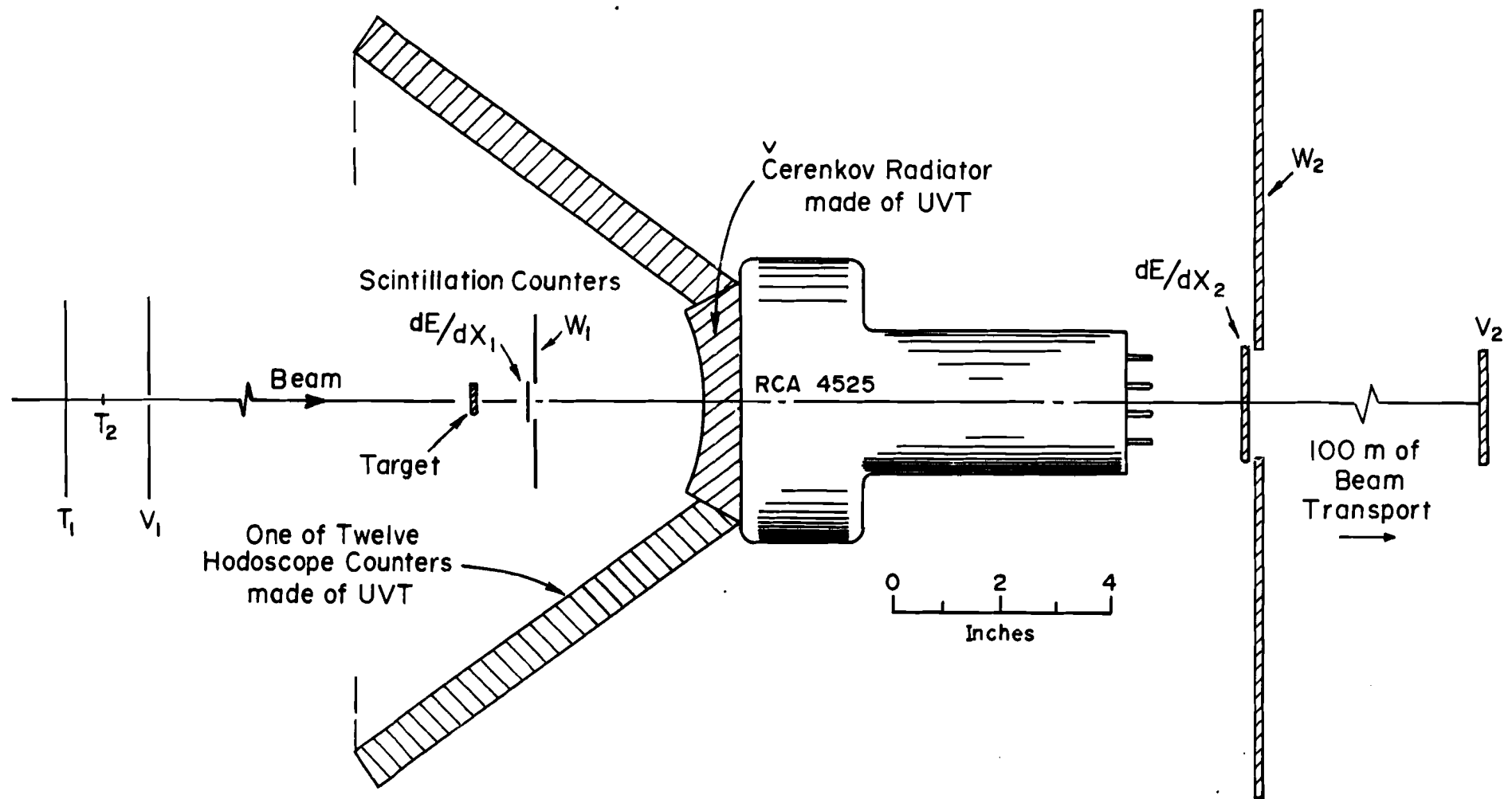
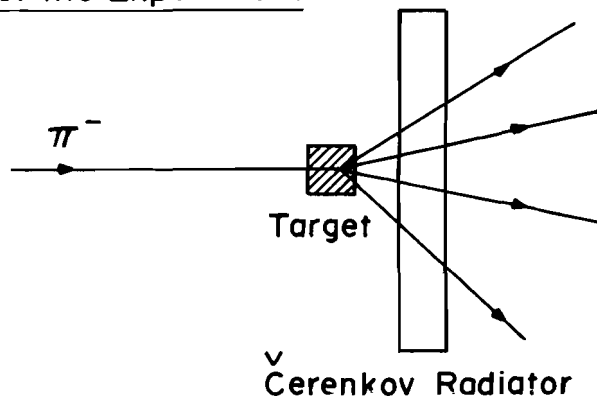


Figure 1

Figure 2
Principle of the Experiment:



Light Output \propto Number of Relativistic Particles

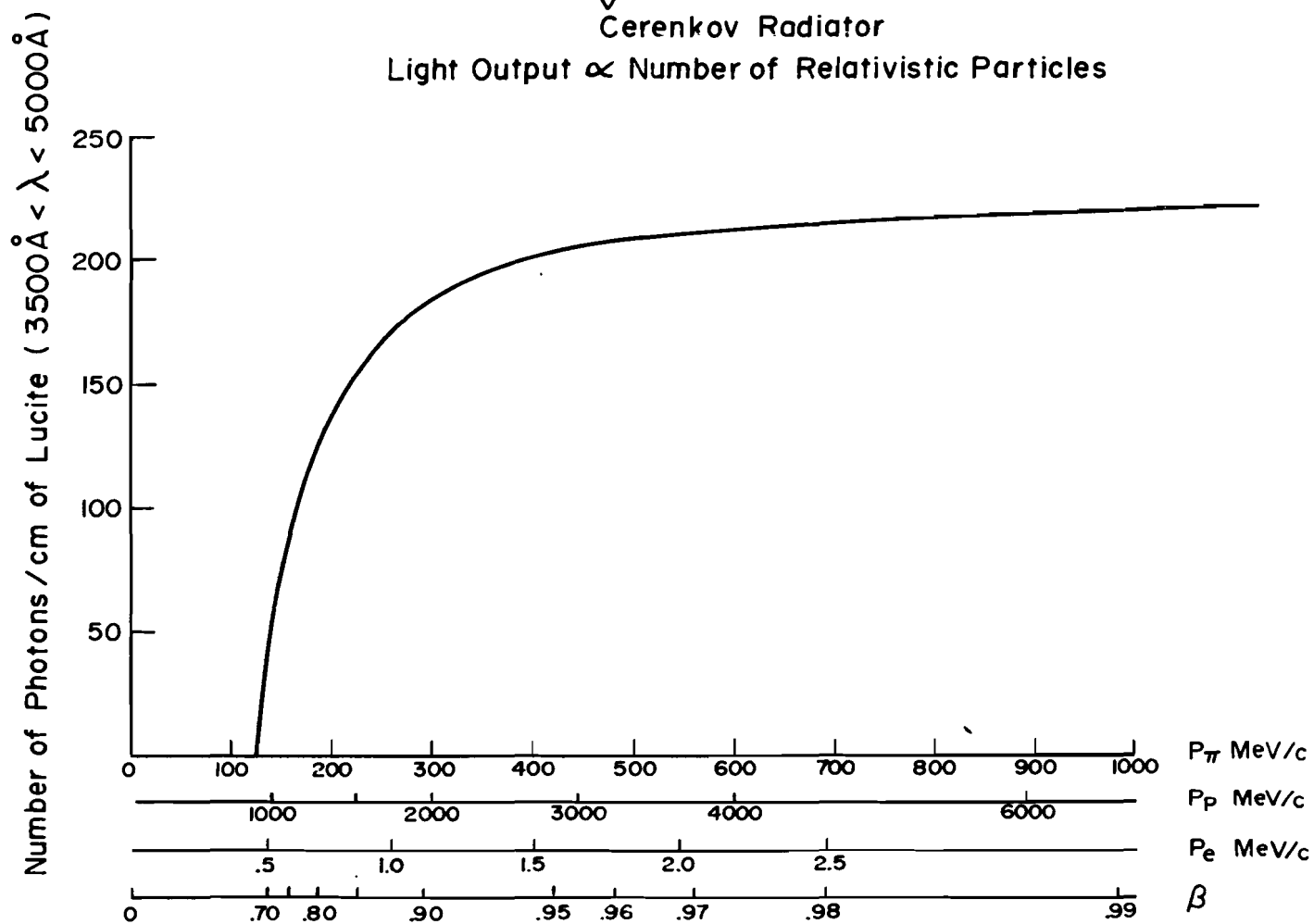
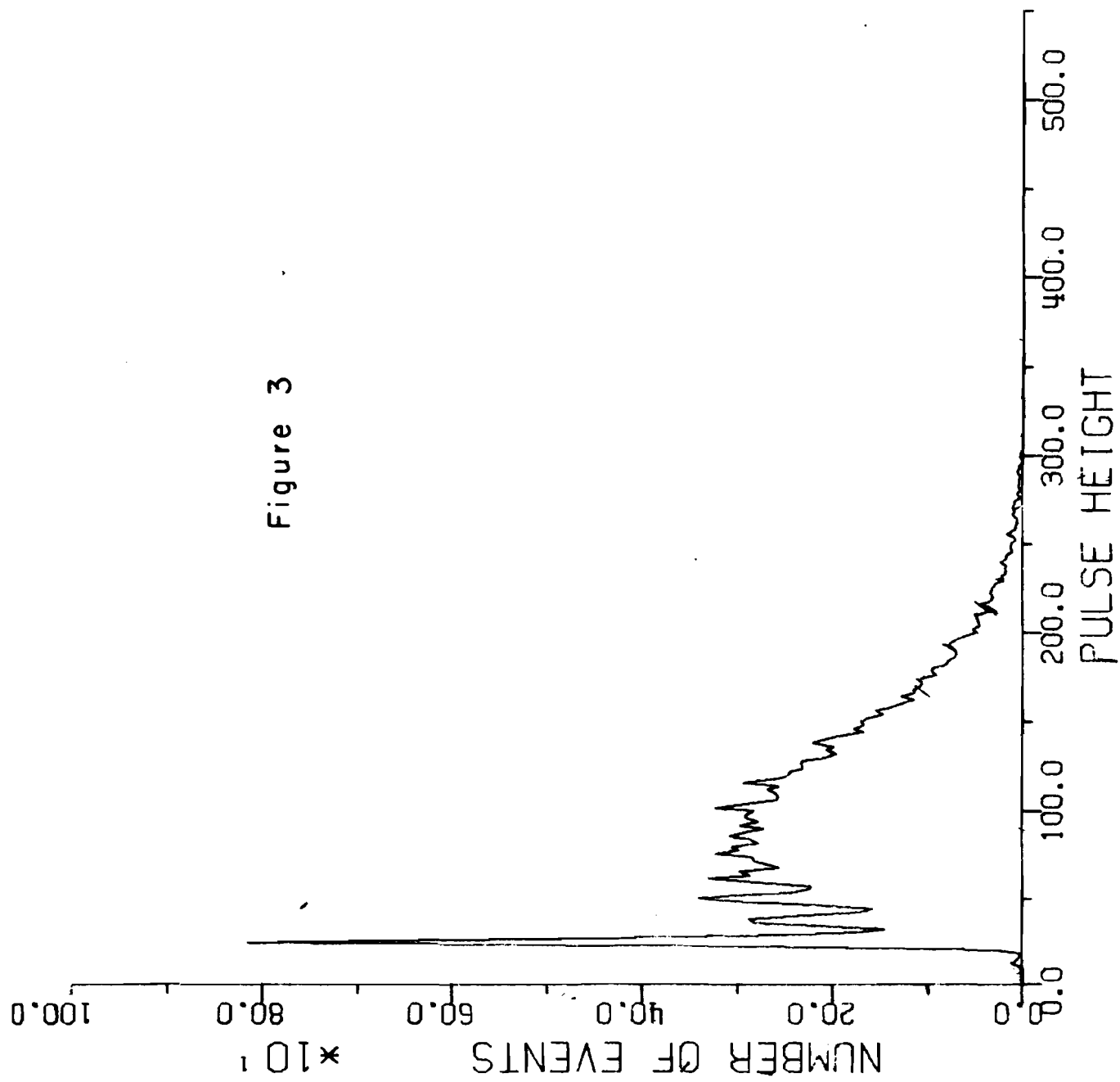
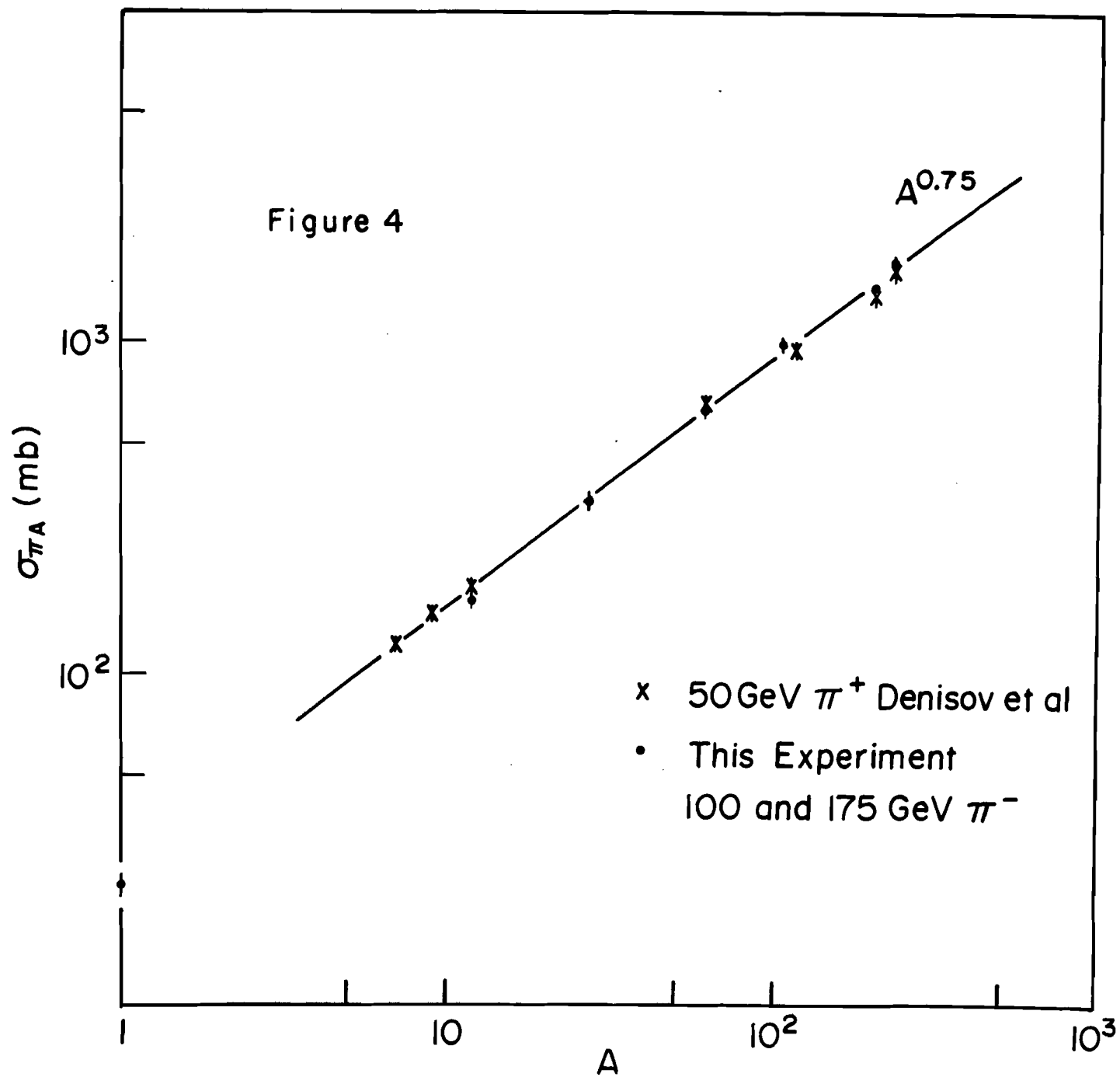


Figure 3





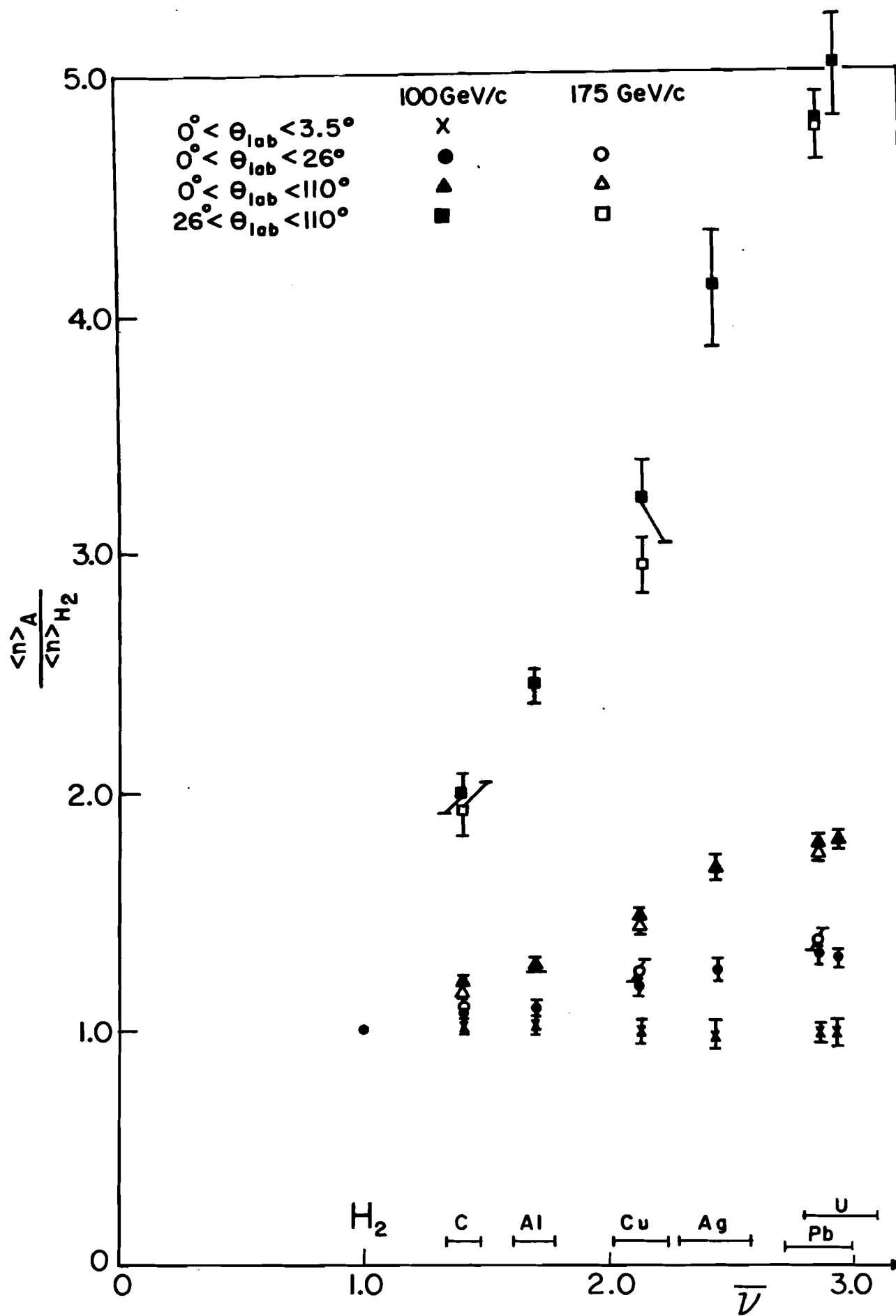


Figure 5

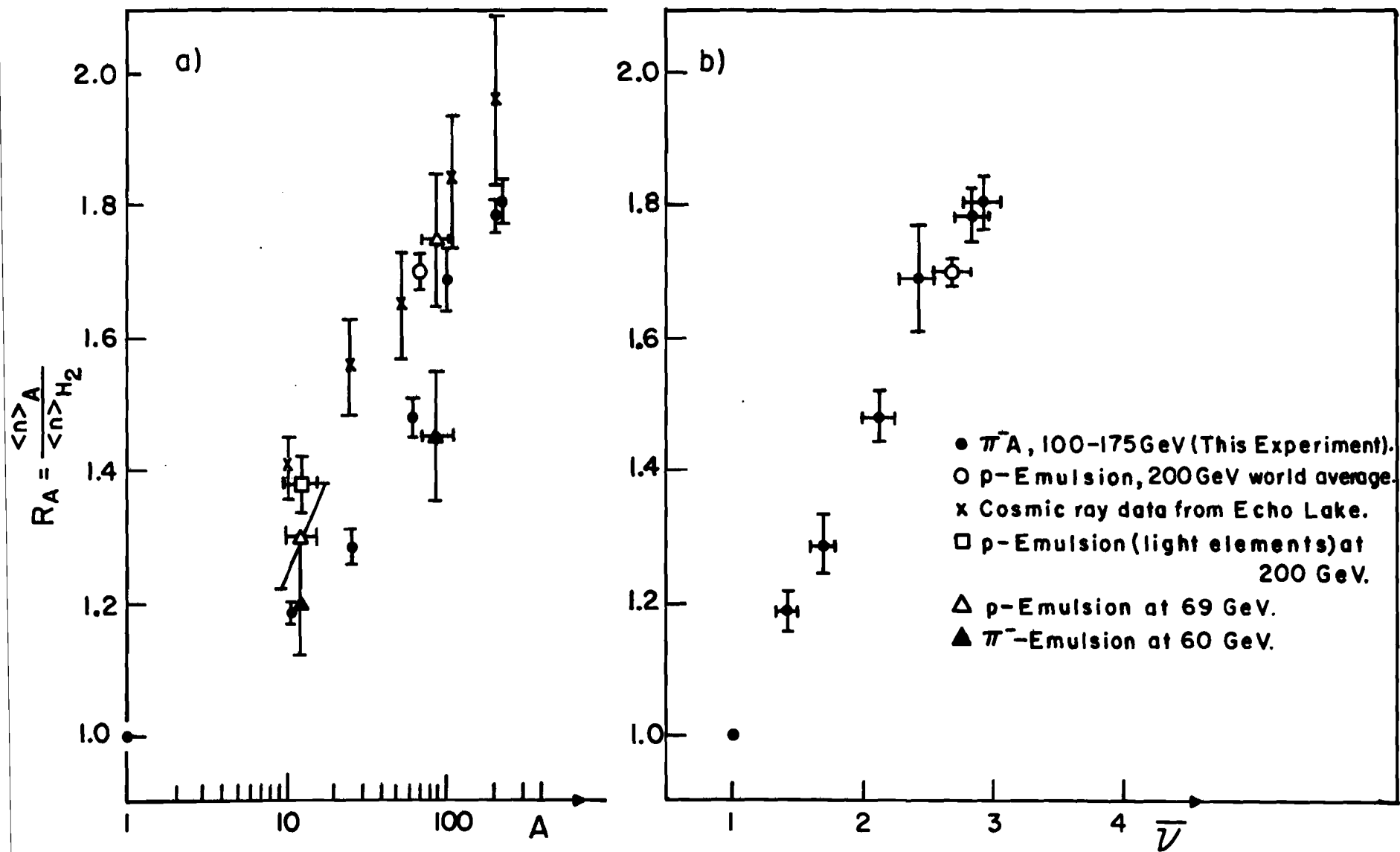


Figure 6

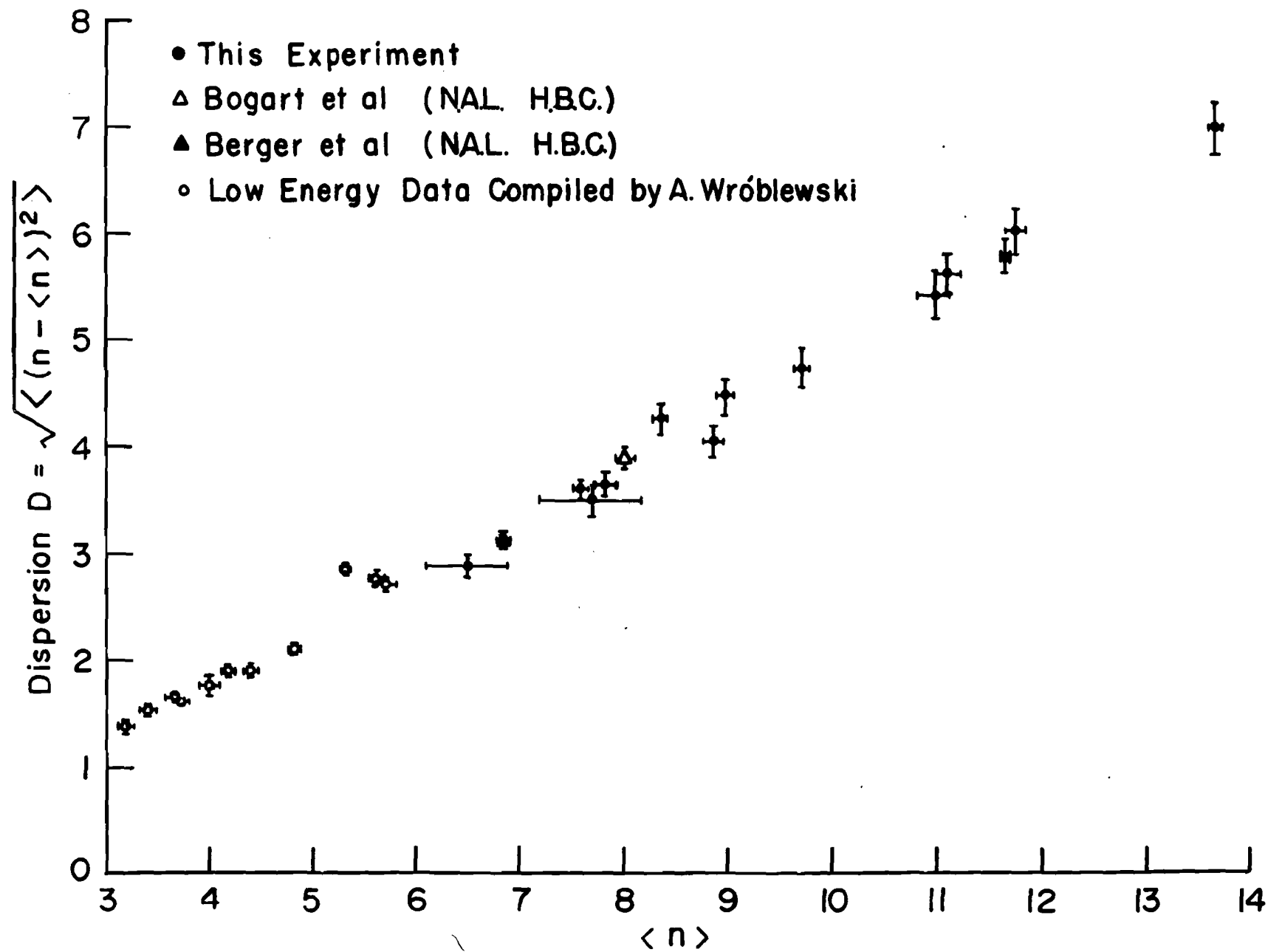


Figure 7

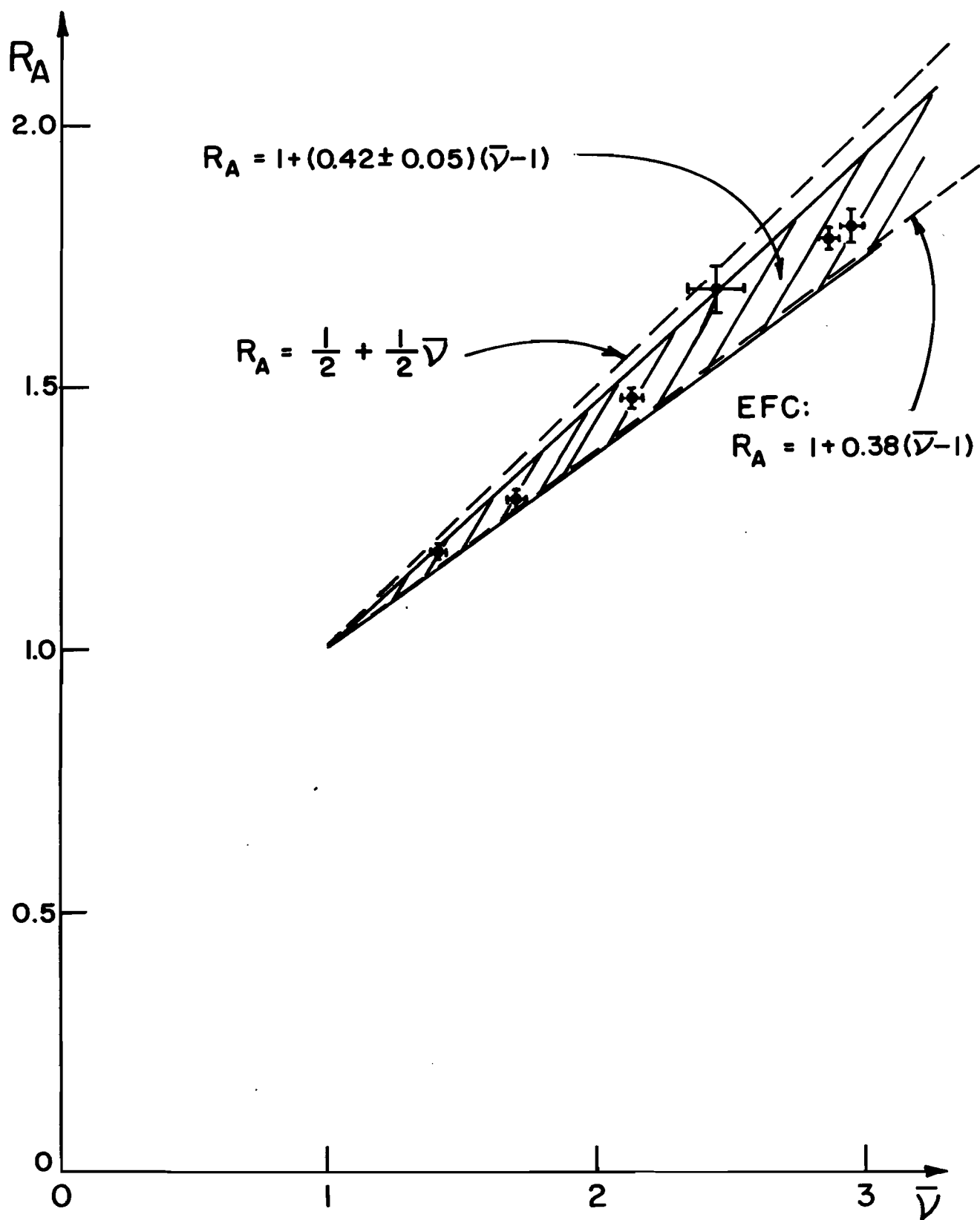


Figure 8

